



SMA-based caterpillar robot using antagonistic actuation

Hangyeol Baek¹ · Nader A. Mansour² · Abdul Manan Khan¹ · Vishwanath Bijalwan¹ · Hussein F. M. Ali^{1,2} · Youngshik Kim¹ 

Received: 31 December 2022 / Accepted: 9 May 2023 / Published online: 18 May 2023

© The Author(s), under exclusive licence to Springer-Verlag GmbH Germany, part of Springer Nature 2023, corrected publication 2023

Abstract

In this research, we present a novel soft robot actuated by shape memory alloy (SMA) springs, which can achieve several different locomotion. The robot can perform inching, crawling, and undulating motions by independently controlling four SMA springs. The SMA springs are arranged in an antagonistic configuration to provide clockwise and counterclockwise motions. Front and rear legs with claws are designed to adjust to friction forces between the robot and the ground, which is essential for the locomotion of the robot. Including one undulatory, three inching, and two crawling locomotions, six locomotion strategies are then implemented in the bang-bang control structure. The applied bang-bang controllers switch control inputs to the robot based on feedback from the orientation angle of the robot body or the SMA temperature. All loco- motion strategies were experimentally validated. The performance of the six locomotion strategies were investigated and compared. Our results show that the fast inching gait can provide a higher velocity and longer tread per gait cycle when compared to the other locomotion strategies.

1 Introduction

Soft-bodied animals such as eels, snakes, and inchworms have drawn the attention of many researchers due to their unique limbless locomotion. Soft-bodied animals use full-body movements for their locomotion such as inching and crawling (Gordon et al. 2017; Brackenbury 1999; Gillis 1997). These animals adopt various locomotion strategies to move and adapt to a given environment (Gordon et al.

2017). For example, a caterpillar can perform various locomotions to escape from threats while sometimes sacrificing stability for a higher locomotion speed (Brackenbury 1999).

There have been many efforts in robotics research to imitate the movements and locomotion of soft-bodied animals. Robot mechanisms should provide higher degrees of flexibility to mimic the full-body motion of a soft animal. However, it is typically difficult to design a hard robot to be highly flexible. Their mechanical structures may also become complicated or heavier since hard robots need additional mechanisms for flexibility such as a series of multiple joints, linkages, and actuators. Thus, soft robots have been investigated to overcome the limitations of hard robots and ultimately to achieve the soft locomotion of soft-bodied animals (Rus and Tolley 2015). A soft robot can be particularly useful in robotic applications with limited workspace where conventional legged or wheeled locomotion cannot be applied.

Soft robots are typically fabricated by using soft materials such as rubber, elastomers, and silicone which can provide higher strains. Thus, soft robots can generate continuous and more natural motions or movements by easily deflecting their soft bodies or changing their shapes similar to soft-bodied animals. For example, a caterpillar-inspired soft robot with a silicone body can achieve crawling and rolling by bending its body considerably (Lin

✉ Youngshik Kim
youngshik@hanbat.ac.kr

Hangyeol Baek
dmb03085@naver.com

Nader A. Mansour
naderabdelwahab@gmail.com

Abdul Manan Khan
abdul.mannan.617@gmail.com

Vishwanath Bijalwan
vishwanath.bijalwan@itgopeshwar.ac.in

Hussein F. M. Ali
hussein.ali@ejust.edu.eg

¹ Department of Mechanical Engineering, Hanbat National University, Daejeon 31458, South Korea

² Department of Mechanical Engineering, Benha Faculty of Engineering, Benha University, Benha 13511, Egypt

et al. 2011). The limbless locomotion of soft robots can provide better mobility and maneuverability in a narrow terrain and small space (Coyle et al. 2018). Soft robots can also provide better compliance and adaptation to given environments compared to traditional hard robots.

Several different actuators have been used to achieve full-body movements of soft robots, which include magnetic actuators (Joyee and Pan 2019), SMA coil actuators (Lin et al. 2011; Koh and Cho 2009), electro-conjugate fluid (Ueno et al. 2014), electric motors (Umedachi et al. 2016), a twisted and coiled actuator (Tang et al. 2019), pneumatic actuators (Branyan et al. 2017) and ionic polymer–metal composite actuators (Yamakita et al. 2005). Previously, Trimmer et al. (2012) demonstrated inching and crawling motion for a caterpillar-inspired soft robot by applying two SMA actuators, one is connected between the head and abdomen of the robot while the other is attached between the abdomen and the tail.

SMA materials have been popularly used as artificial muscles in robotic systems since they contract and relax similar to muscles. Some advantages of SMAs include silent operation, compliance, larger deformation, lightness, and compactness. SMAs can also provide larger forces with lighter weight. SMAs can easily be activated by applying a low electric voltage. SMAs can also be trained in linear, coil, and other shapes by heat treatment.

In this study, SMA coil springs are used similar to muscles to achieve full-body soft motion by actuating two body segments (front/anterior and rear/posterior) of the robot. To this end, each body segment can be contracted and relaxed actively by using a pair of two coil springs in an antagonistic configuration. Respective front and rear SMA actuator pairs are applied to generate motion of the front and rear body segments. As a result, we can ultimately achieve full-body soft motion and locomotion gaits similar to small soft-bodied animals by using coordinated control of these SMA actuator pairs.

Inching and crawling locomotion have typically been adopted for soft robots. In these locomotion methods, a robot repeats contraction and relaxation of its body to make a movement while sticking a particular part of the body on the ground and slipping the other body parts. Particularly, some body appendages such as claws or hairs that can grip the ground are used to anchor a body part to the ground such that the other body part(s) can be propelled forward against an anchored body part. Locomotion strategies for a soft robot are generally developed based on this moving principle. However, locomotion gaits should be modified for each robot system since robot gaits are limited by the mechanical constraints and design of a robot (Trimmer et al. 2012). Furthermore, locomotion patterns can be modified easily by changing the actuator power, gait timing, and gait transition.

In Table 1, we summarize the design features of several different caterpillar-like robots and their locomotion methods. Bodies of these robots are typically fabricated by using soft materials; rubber bellows (Ueno et al. 2014), silicone (Tang et al. 2019), flexible polymer (Joyee and Pan 2019), and TPU (Thermoplastic Polyurethane) in this research. In the aforementioned research, the first mode shape of a body structure is also traditionally used to achieve their locomotions. Thus, a single actuator or a pair of two actuators is used to generate unidirectional bending motions. For instance, GoQbot uses two SMA spring actuators in series to generate a curling motion. Further, multiple different types of appendages are simultaneously used in most research to provide friction and/or gait stability for their robots.

Several researchers present magnetically actuated soft robots to provide multi-directional bending motion. Wenqi Hu et al. (2018) use soft active materials that can generate various shapes to provide walking, crawling, landing, climbing, and jumping. Stretchable origami structures are used for omnidirectional bending and twisting in Yamakita et al. (2021). Ju et al. (2021) use soft magnetic composite materials to provide rolling locomotion. These magnetically actuated robots may be suitable for medical applications. However, because these robots should be actuated on the magnetic field, their applications are critically limited.

The objective of this research is a design of an SMA-based soft robot which provides multi-directional bending motion. Our soft robot can perform soft motion and locomotion such as inching, crawling, and undulating with a simple structure. The body of the robot is made of Thermoplastic Polyurethane (TPU), which provides both flexibility and elasticity. The robot is actively actuated in a bidirectional way (i.e., contraction and relaxation motions) by using two actuator pairs of SMA coil springs in an antagonistic configuration. Active and bidirectional actuation of the robot can lead to a faster system response. An SMA actuator pair consist of two coil springs; one is mounted above the robot body whereas the other SMA is attached below the robot body. We implement the first pair of SMA actuators between the front part of the body and the middle of the body. The second actuator pair is then attached between the middle of the body and the rear part of the body. Furthermore, two legs with arc-shaped claws are attached to the front and rear body parts to better facilitate the stick and slip phenomenon during locomotion. As a result, the robot can generate undulating or soft motion by using these minimum two pairs of SMA actuators. We implement a undulatory motion, and several inching and crawling locomotions (anterior inching, posterior inching, fast inching, crawling, and faster crawling) similar to Trimmer et al. (2012).

Table 1 Comparison of caterpillar robot design

Caterpillar robot	No. of actuators	Material of actuators	Material of robot body	Appendages for grip	Locomotion methods
Ueno (2014)	1	Electro- conjugate fluid	Rubber bellows	Silicone rubber for high friction, metal plate for low friction	Inching
Tang (2019)	1	Twisted nylon fiber and nickel wire	silicone	Paper clips for low friction, hot melt glue for high friction	Inching
GoQbot (Lin et al. (2011))	2	SMA spring	Silicone	Cylindrical shape hammer head, wedge legs, tail skids	Inching, crawling, rolling
Joyee (2019)	2	Permanent magnets	Polymer	Magnetic particle-polymer composite	Inching
Our robot	4	SMA spring	TPU	Arc-shaped claws	Inching, crawling, undulating

Furthermore, we investigate the deflections of the robot body using a finite element method and simplified beam analysis. Our finite element simulation and analytical results confirmed that the robot can perform the expected soft motion as designed. Finally, we experimentally validated the design of our soft robot and soft locomotion strategies. To control the motion of the robot, we use bang-bang controllers. The experimental results also confirmed that the robot can perform soft locomotion and motions as designed. Our demonstrated motions can easily be adjusted for different applications and scenarios. Particularly, a vertical undulation can be used to mimic the snake-like undulatory motion or jellyfish motion.

- In this research, we present a simple but novel soft robot mechanism actuated by using two sets of SMA pairs in antagonistic configuration. Our main contributions include an SMA-actuated robot mechanism, coordinated manipulation of antagonistic SMA actuator pairs for soft locomotion, and experimental validation of soft locomotion. We particularly investigate uses of the first or second mode shape of the beam to generate undulating gaits for soft locomotion. We also study more controllable manipulation of body shapes for soft locomotion by using two antagonistic SMA pairs. We plan gait cycles and desired body shapes for our robot. The front and rear segments of the robot body are independently actuated in bi-direction (clockwise and counterclockwise) by using antagonistically arranged SMA actuators. As a result, our robot generates more sophisticated gaits by coordinating bidirectional bending motions in the first or second mode. Finally, we verify experimentally the proposed robot performs soft motion and locomotion such as inching, crawling, and undulating motions.

The remainder of this paper is structured as follows. In Sect. 2, we discuss the design and mechanism of the soft robot. In Sect. 3 we describe the locomotion strategies of

the robot that can mimic the mobility of an inchworm or eel. The control sequences of the robot are also presented. In Sect. 5, we present the simulation-based analysis and experimental results. Finally, the conclusions of this study are provided in Sect. 6.

2 Design of the bio-inspired soft robot

Soft-bodied animals like caterpillars and inchworms use limbless locomotion such as inching and rolling in which their full-bodies are used to generate their movements and motions. Soft animals typically repeat bending over and stretching out their bodies to generate propulsive forces while anchoring their body segment to the ground using appendages shown in Fig. 1. Appendages like claws, hairs or scales are generally used to hold a body segment steady on the ground while moving the other body segment(s) forward. For instance, an inchworm actively changes contact interactions with surfaces using claws. The bending motion of an eel produces a locomotory wave to move in a fluid (Gillis 1997). The bending motion of a caterpillar used for its locomotion is produced by adjusting its muscle power for each body segment. The main

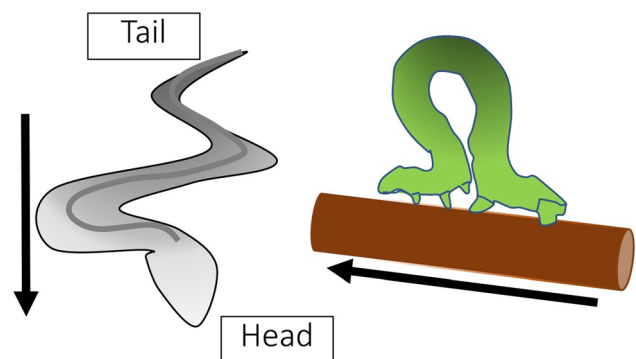


Fig. 1 Bending movement

structure and actuation of our robot are inspired by the aforementioned soft bodied animals. The robot body is fabricated using soft materials with a higher strain and elasticity. SMA springs are then used similar to muscles to contract and relax the soft body of the robot. The mechanical structure of the robot is shown in Fig. 2.

In this study, we use simple bending modes of the body frame to achieve full-body locomotion of the robot. The robot body is thus made of thermo-plastic polyurethane elastomers (TPU) with a higher softness and elasticity. As a result, the robot body can easily deflect by applying external forces and restore its original shape when removing those external forces. SMA spring actuators are then used to deflect the robot body. SMAs can be activated easily by applying electric current inputs and provide sufficient forces to bend the robot body. We use four SMA springs (0.020 inch-thick Flexinol wire with a 0.136 inch helical diameter). The inactivated length of the SMA actuator is 1.732283 inch, which is less than one-half the length of the body. The minimum length of the SMA is 1.299213 inch when activated. Note the total length of the robot is 14 cm. TPU can withstand high temperatures of 140–150 °C, which is higher than the transition temperature of the SMA. Also note the SMA used in this study provides maximum contraction at 90°C to 100°C.

Since the first and/or second bending modes of the robot body are used for locomotion, the SMA actuators are connected to the front and rear body segments. To this end, six rigid square blocks 0.19685 inch thick are attached to three locations (right, middle, and left) in the robot body shown in Fig. 2. Both ends of an SMA are fixed to these blocks. As a result, bending motions of the front and rear body segments can be generated independently. The two SMA actuators are arranged in an antagonistic configuration to provide bidirectional (clockwise and counterclockwise) bending deflections for a body segment. In this antagonistic configuration, one SMA is attached to the top of a body segment whereas the other is attached to the bottom. The respective front (SMAs 3 and 4) and rear

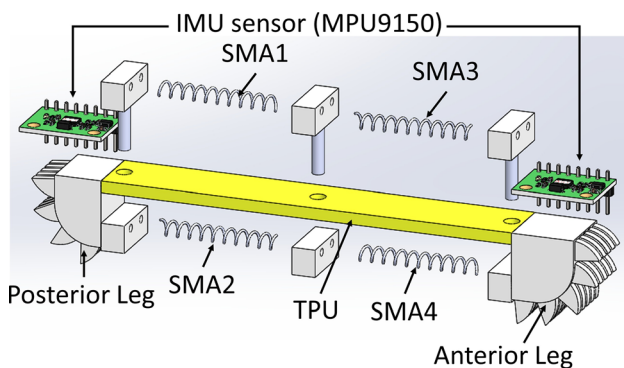


Fig. 2 Mechanical structure of the robot

(SMAs 1 and 2) actuators can be actuated independently to deflect and stretch the front and rear body segments. As a result, full-body undulatory locomotion can be achieved by applying coordinated control of these front and rear SMAs. Locomotion strategies for the robot were then investigated to determine the coordinated SMA actuation. Our simple bending mode-based locomotion strategies simplify control of the robot since only the first or second bending mode of the entire body frame is used. The locomotion gaits of the robot are achieved by coordinating the simple bending mode shapes of the front and rear body segments.

The caterpillar uses some legs/appendages for a strong grip on the ground to provide traction while moving forward. Similarly, the legs of our robot are designed to have several arrays of arc-shaped claws which function like the claws of an animal to provide a strong grip on a given surface. The legs of our robot are made of Poly Lactic Acid. Arc-shaped metal claws are then attached to the tips of the legs shown in Fig. 3 such that these claws increase the traction forces considerably on the ground. By adopting the arc-shaped design, a claw can slide easily on the ground when it is rotated counterclockwise. However, the claw is anchored to the ground when it is rotated clockwise. IMU (MPU9150) sensors are mounted on the anterior and posterior legs of the robot to measure the orientation angles of the front and rear end points of the robot body. These orientation angles are then used to provide feedback for a locomotion controller.

3 Locomotion strategies and operating principle

3.1 Locomotion strategies

Animals with soft bodies such as an inchworm and a caterpillar generate locomotion gaits undulating their whole bodies. Caterpillars and inch worms push and pull their bodies while actively changing the contact areas and frictional forces between their bodies and the ground. Particularly, a caterpillar crawls by alternatively

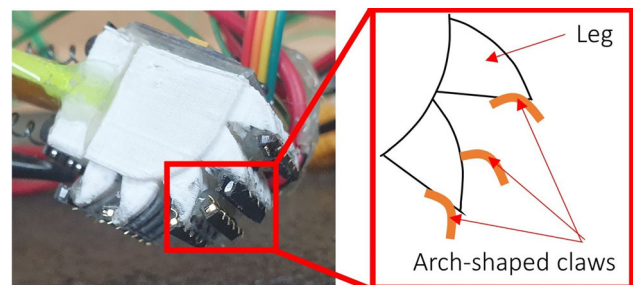


Fig. 3 Anterior leg and claws

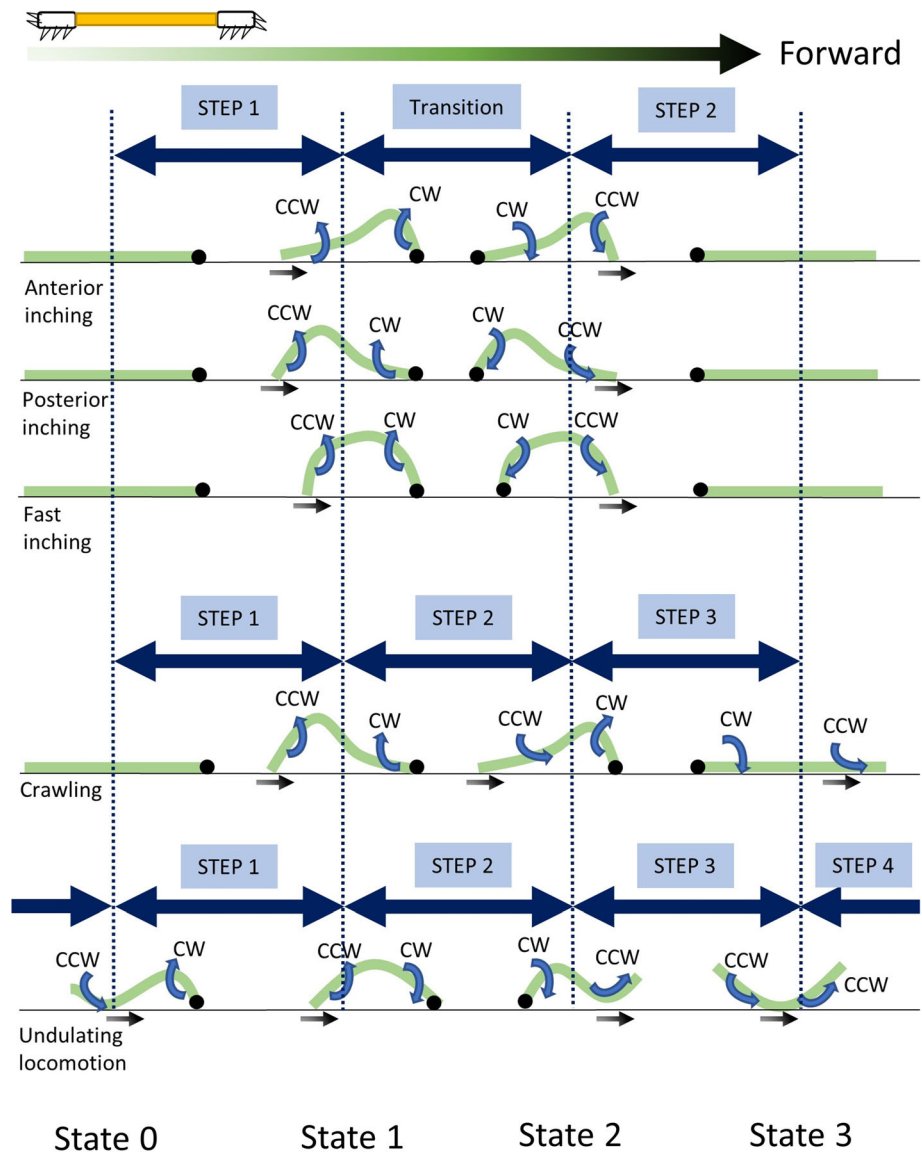
contracting/bending and stretching its body while grasping the ground. In this section, we discuss five different whole-body locomotion strategies (anterior inching, posterior inching, fast inching, crawling, and undulating), which are all applicable to our soft robot. Fig. 4 shows the gait maps for locomotion.

In the anterior inching, the robot first pulls the rear body forward while bending the front body. Thus, the anterior leg is rotated clock-wise such that its claw is locked on the ground. The posterior leg is rotated counterclockwise such that its claw slides on the ground. Note the friction between the claws and ground is significantly reduced when the leg or claw rotates counterclockwise. Also note the friction significantly increases when the leg or claw rotates clockwise such that the claw is locked on the ground similarly behaving like a fixed pin joint. Next, the robot body is

stretched again while the rear claws are locked, and the front claws slide on the ground. Note the anterior and posterior legs are rotated counterclockwise and clockwise, respectively, during this stretching phase. As a result, the robot moves forward. The resulting moving distance of the robot is proportional to the amount of the bending displacement of the robot.

In the posterior inching, the rear body is bent and pushed forward simultaneously while the front body is rotating clockwise about an anchor point generated by the front claws. When the body is stretched again, the front body moves forward while the rear body is rotating clockwise about an anchor point supported by the rear claws. As a result, the robot travels forward depending on the amount of bending displacement of the rear body.

Fig. 4 Locomotion strategies for a soft robot. A robot moves from left to right. Black dots indicate the anchor points of the robot on the ground. Red arrows illustrate the contraction of the robot body whereas blue arrows illustrate relaxation



In our crawling, we combine posterior and anterior inching locomotion gaits sequentially to increase the travel distance. The resulting locomotion gait pattern is similar to the shape of a wave propagation in which a wave transfers from the rear part of the body to the front part of the body. The transition of the wave pattern can be adjusted for faster movement.

In the fast inching, the whole (front and rear) body of the robot is bent in a curved shape while the front leg is locked on the ground. The robot is stretched again while the rear leg is locked on the ground. Likewise, the travel distance of the robot is proportional to the bending displacement. The fast-inching gait can provide a higher speed when compared to the aforementioned inching gaits since it can increase the travel distance by bending the whole body simultaneously. The fast-inching gait can also increase the vertical displacement such that its use may be limited in a narrow space.

The undulatory locomotion uses a sinusoidal wave pattern to move forward simultaneously coordinating locking and unlocking of each leg shown in Fig. 4. This locomotion is commonly used in many animals without limbs. For example, snakes or salamanders use this locomotion when they travel on land or swim in water. A undulatory wave propagates from the front body to the rear body while first locking the front leg and unlocking the rear leg. The front leg is then released and pushed forward while the rear body is locked. As a result, the robot travels a distance which is proportional to the applied wave length.

3.2 Operating principle

In this study, we designed a soft robot that can perform several different whole-body locomotions simultaneously. Several different locomotion gaits were then applied to the robot. The motion and locomotion characteristics of the robot can be varied by simply changing the input power to the actuators and the control time in a gait pattern. The robot is initially in the straight resting position where it is simply supported by the two legs located at the ends of the body. The undulatory movement of the robot is achieved by coordinating the actuation of the four SMA springs. Each body segment is actively bent or passively deflected to produce a specific gait configuration. During the active bending phase, the front leg is locked whereas the rear leg is unlocked such that the rear leg moves forward (right) on the ground. During the stretching phase where all the SMAs are off, the robot body is stretched to its original shape due to elasticity and gravity. Since the rear leg is locked on the ground, the front leg then moves forward.

The operating principle of the robot is based on active bending and restoring the forces/torques in the robot body by locking and unlocking the contact points of the legs.

Total travel distance is determined by the amounts of bending and stretching deflection. Note that the friction forces of the legs vary depending on the orientation of the claws since the friction coefficients of the claws change as the contact angles between our arc-shaped claws and the ground change. When the leg rotates in the clockwise direction, the friction coefficient of the claw increases such that the leg is anchored during rotation. However, when the leg rotates in the counterclockwise direction, the friction coefficient of the claw decreases such that the leg can easily slide to the right direction during rotation.

While the robot moves, one of the front and rear claws is anchored to the ground to provide traction whereas the other claw is in smooth sliding contact with the ground. The design of the arc-shaped claws is thus to increase or decrease the friction force on the ground as the orientation of the robot body changes during locomotion. This arc-shaped design helps the robot obtain the desired gaits by keeping the ground contact parts of the robot locked or unlocked on the ground. An unlocked contact part can slip smoothly on the ground by a small horizontal push or pull force. The angle of the claws attached to the leg was determined experimentally to increase the locking and unlocking capabilities.

The front (SMAs 3 and 4) and rear (SMAs 1 and 2) actuators are arranged in an antagonistic configuration to generate a faster robot motion. As soon as one SMA is off, the other actuator in an antagonistic configuration is on immediately to increase the next phase transition speed of the robot in our locomotion strategies.

4 Finite element modelling of the soft robot

As described earlier, our robot body consists of a continuous beam actuated by two SMA spring pairs. Thus, the robot body can be divided into two segments (i.e., front body and rear body segments) considering the actuating locations and resulting deflection. By actuating the SMA springs connected to both ends of each segment, the deflection of each segment changes, and the robot moves ultimately. The deflection generated at the center point of each segment is modelled as the deflection generated by the moments at the midspan of a simply supported beam. Fig. 5 shows a simplified model for the front and rear body segments of our robot. The maximum deflection is calculated by

$$\delta_{max} = \frac{ML^2}{8EI} \quad (1)$$

where M is the bending moment; L is the length of the beam ($L = 50$ mm for each segment); E is the Young's modulus of elasticity ($E = 26$ MPa for the TPU material),

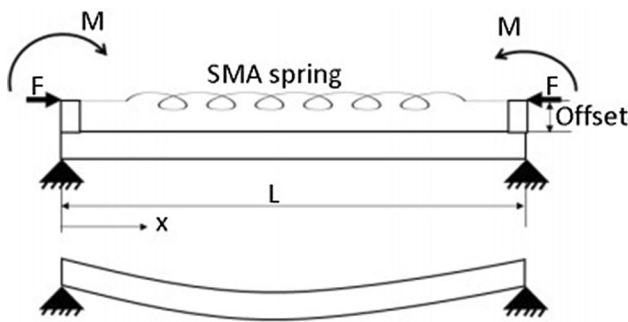


Fig. 5 Simplified model of the simply-supported beam

and I is the moment of inertia of the beam section. The bending moment M is calculated based on the force generated by the SMA spring at an offset of 2 mm. The maximum force generated by the SMA ($F = 15$ N) was determined experimentally. Fig. 6 shows the experimental setup used to determine the force generated by the SMA. The actuated SMA spring was installed between a force sensor (Model: BCL-3L) and a moving element driven gradually by a stepper motor. Considering that the robot body is 3D- printed using TPU with 30% fill, the cross section of the TPU body of the robot is not completely solid and is not exactly hollow as well. Hence, the moment of inertia I is calculated assuming that the cross section of the TPU body is an average value between a solid beam (Eq. 2) and a hollowed beam (Eq. 3).

$$I_{solidbeam} = \frac{BH^3}{12} \tag{2}$$

$$I_{hollowbeam} = \frac{BH^3}{12} - \frac{bh^3}{12} \tag{3}$$

where, ($B= 16$ mm) and ($H= 3$ mm) are the width and thickness of the body are $B = 16$ mm and $H = 3$ mm, and the width and thickness of the inner hole of the hollow beam are $b = 15$ mm and $h = 2$ mm, shown in Fig. 7.

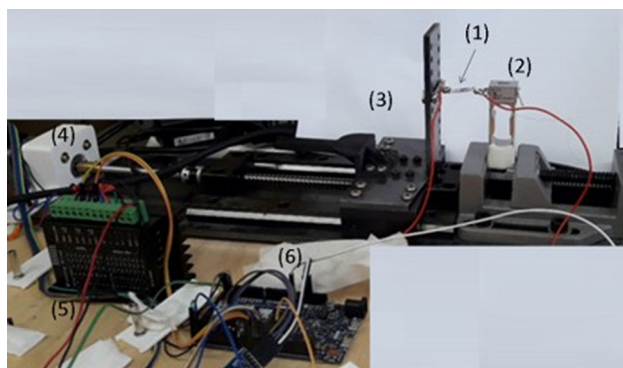


Fig. 6 Experimental setup used to find the force generated by the SMA spring. (1) SMA spring (2) force sensor (Model: BCL-3L) (3) moving element (4) stepper motor (5) motor driver (6) Arduino due microcontroller

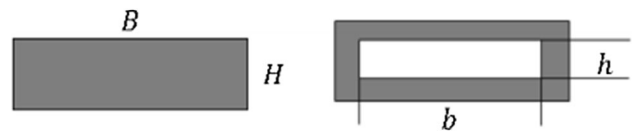


Fig. 7 Cross-section dimensions of each segment

Hence, the maximum deflection obtained using Eq. (1) was 11.6 mm at the midspan of each body segment.

Furthermore, we verified our simplified model through Finite Element Analyses (FEA). We applied two different mode shapes to simulate the body deflections in FEA. We modeled the robot as a simple beam structure with three support blocks (right, middle, and left) similar to the legs and actuator support in our robot. These support blocks were used to simulate the interaction of the robot with the ground. We studied different cases of the robot including anterior, posterior, and fast inching, and undulating locomotion. Figure 8 depicts the model of the robot used in anterior and posterior inching. In this model, the right end of the robot is fixed to simulate grasping the ground. The left end is then defined as a cylindrical support with a sliding contact edge between the robot and the ground. In this case, the forces exerted by the SMA springs are applied on the lower part of the left and middle support blocks. Similarly, deflection profiles in fast inching and undulation are shown in Figs. 9 and 10, respectively. In Fig. 9, the right and left ends of the robot are modeled as a cylindrical support with fixed axial boundaries. Forces exerted by the SMA springs are applied to the lower side of the two support blocks.

Similarly, the undulation is modelled, as shown in Fig. 10, by applying SMA forces at the lower left and the upper right of the support blocks.

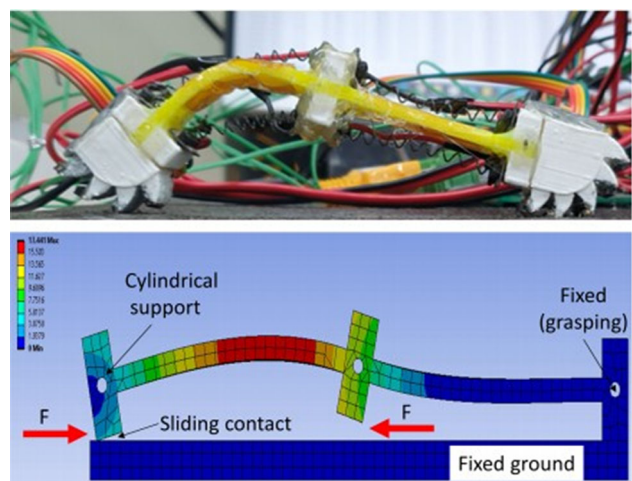


Fig. 8 Model of the robot in Anterior/Posterior inching

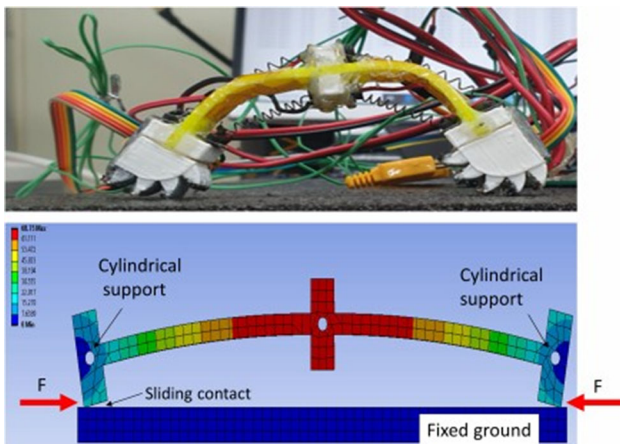


Fig. 9 Model of the robot in fast inching

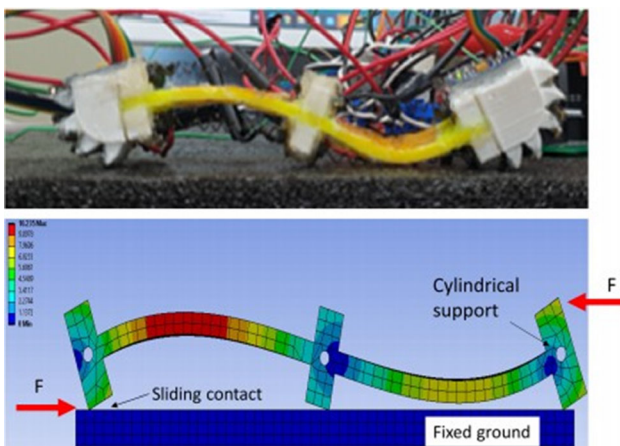


Fig. 10 Model of the robot in the undulation

5 Experiment

5.1 Experimental setup

Experiments were conducted to validate the design and locomotion capabilities of our soft robot. Our experimental setup is shown in Fig. 11. The robot was tested on a flat surface with high friction to highlight the locomotion strategies and their features. We use electrical power to activate the SMA actuators. In this case, we provide electric currents of 2 A for the SMA actuation. SMA actuators are then deactivated by using natural convection air cooling. The ambient air temperature was 25–26 °C. SMA actuator drivers consisting of relay circuits are used to selectively provide control commands from a microcontroller to the front and rear actuators shown in Fig. 12. An arduino microcontroller is used to implement the sensing, control, and locomotion algorithms in the robot. IMUs and thermocouples are used to provide feedback signals for robot control. MAX6675k-type thermocouples are used as

shown in Fig. 11 to measure the temperatures of the SMA actuators. Furthermore, heat-resistant tape is attached onto the surfaces of the robot body to prevent thermal damage to the robot in the case of the SMA actuators overheating.

5.2 Controller implementation

A bang-bang control structure is used to implement the locomotion strategies for our soft robot. The SMA temperatures or body orientation angles can be used as feedback signals in our control structure.

A temperature feedback-based bang-bang control structure is used to achieve the inching and crawling locomotions for our soft robot. In our bang-bang control algorithm, control inputs provide the low and high states of the current inputs to the SMA actuators similar to ON-OFF switches. In our case, electrical power of 10 V and 2 A is used to operate the robot. Thus, a current of 2 A is supplied to an actuator to turn it on whereas 0 A is supplied to turn it off.

In the bang-bang control structure for the inching and crawling locomotions, the control sequences of the SMA actuators, presented in Table 2, are predetermined for each locomotion state according to our locomotion strategies shown in Fig. 4. Initially, all SMAs are off. We then turn on a particular SMA actuator based on an applied locomotion strategy. Next, we switch on another SMA in sequence while turning off the previously activated SMA when this activated SMA reaches its full transition temperature of 90 °C. Note an SMA reaches its maximum strain at its transition temperature which provides a sufficient bending motion for robot locomotion.

The undulating locomotion is achieved by applying a bang-bang controller with orientation angle feedback. The orientation angles of the front and rear ends of the robot body are measured by IMU sensors. The bang-bang controller switches the control commands between two states (that is, 0 A for off and 2 A for on) of electrical current. Thus, 2 A is supplied to an active SMA actuator according to the predetermined control sequences of the SMA actuators, presented in Table 2, until an orientation angle of the robot body reaches a desired angle.

5.3 Experiments: inching and crawling locomotions

In this study, the robot can perform several different soft locomotion. Inching and crawling capabilities were first investigated experimentally applying five different locomotion strategies as discussed in Sect. 3. Inching and crawling motions are achieved by using the bang-bang controllers which switch control commands from a gait state to the next gait state based on the SMA temperature

Fig. 11 Schematics of the SMA actuator drivers

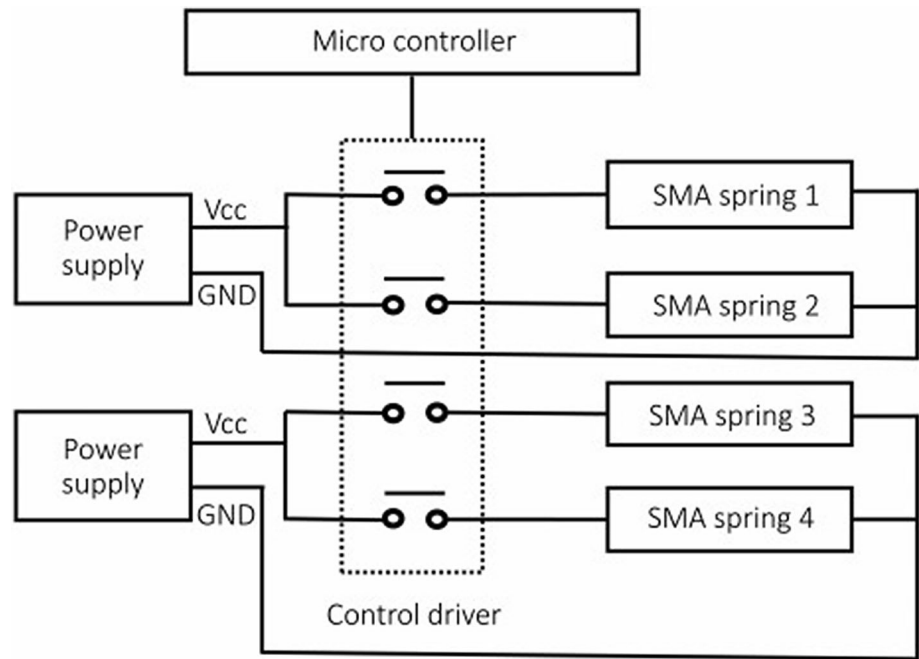
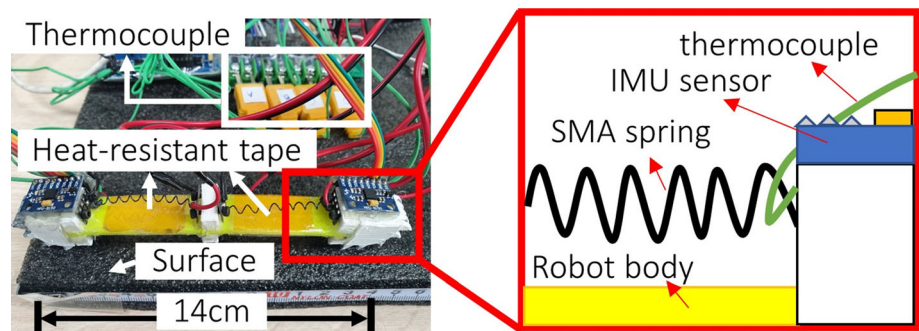


Fig. 12 Experimental setup: actual soft robot on a flat surface



feedback signals. Table 2 shows the control sequences of the SMA actuators proposed for the inching and crawling locomotions. All SMA actuators are initially off. A corresponding SMA actuator is then on as scheduled until this SMA actuator is heated up to its transition temperature of 90 °C. The inching and crawling locomotions of our soft robot were experimentally verified. Our experimental results are discussed in this section.

The robot rested on a flat terrain with higher friction at an initial gait state. Inching (anterior, posterior, and fast) and crawling (basic and faster) locomotion gaits were implemented in the robot shown in Fig. 4 and Table 2. Experimental results (robot gaits and sensor measurements) obtained from inching and crawling tests are shown in Figs. 13, 14, 15, 16, 17, 18.

Figure 13a shows the sequential snap shots from the experimental results of the anterior inching locomotion where the front body segment is significantly bent. The robot rests straightly on the ground in the initial State 0. In Step 1 for contraction, the rear leg slides forward while the

front leg is locked on the ground applying electrical current to SMA 4 located below the front body. In the transition state between States 1 and 2 where the temperature of SMA 4 reaches its transition temperature and maximum deflection is simultaneously obtained, SMA 4 is then deactivated immediately to be relaxed for Step 2 whereas its antagonistic actuator SMA 3 is activated for faster relaxation of the front body. In the final State 3 where the robot body returns to its original straight shape, SMA 3 is off. If the body is relaxed by natural cooling of SMA 4 in Step 2 without using its antagonistic SMA 3, the time elapsed between States 2 and 3 increases more than 10 seconds. Figure 13b shows the orientation angle measurements of the anterior (or front) and posterior (or rear) legs during a single cycle of anterior inching. These results indicate that the front body segment is bent more than the rear body segment. The maximum deflection occurs during the state transition between States 1 and 2 as mentioned. Temperature measurements of the four SMA actuators, depicted in Fig. 13c, show the SMA 3 and 4 actuators are activated and

Table 2 Proposed SMA actuation plan for inching and crawling

Gait	State	SMA1	SMA2	SMA3	SMA4
Anterior inching	0	OFF	OFF	OFF	OFF
	1	OFF	OFF	OFF	ON
	2	OFF	OFF	ON	OFF
	3	OFF	OFF	OFF	OFF
Posterior inching	0	OFF	OFF	OFF	OFF
	1	OFF	ON	OFF	OFF
	2	ON	OFF	OFF	OFF
	3	OFF	OFF	OFF	OFF
Crawling	0	OFF	OFF	OFF	OFF
	1	OFF	ON	OFF	OFF
	2	OFF	OFF	OFF	ON
	3	OFF	OFF	ON	OFF
Fast inching	0	OFF	OFF	OFF	OFF
	1	OFF	ON	OFF	ON
	2	ON	OFF	ON	OFF
	3	OFF	OFF	OFF	OFF

deactivated as proposed by our gait plans shown in Fig. 4 and Table 2.

Sequential snap shots obtained from the experiments of the posterior inching locomotion are shown in Fig. 14a. Posterior inching considerably bends the rear body segment of the robot from a straight posture of the initial Step 0.

Thus, SMA 2 is activated in Step 1 such that the rear leg slides forward while the front leg is anchored to the ground. During the state transition from contraction to relaxation, SMA 1 is activated for faster relaxation whereas SMA 2 is off. Our results show that the relaxation speed from States 2 and 3 of posterior inching is faster than that of anterior inching by 2 seconds. This faster relaxation is achieved since the sliding friction of the front leg during relaxation of Step 2 in posterior inching is smaller than that in anterior inching. In our case, the front leg rotates 18.2° clockwise, shown in Fig. 14b, in States 1 and 2 of posterior inching whereas the front leg rotates 51.9° clockwise, shown in Fig. 13b, in anterior inching. Thus, normal force acting on the front leg in posterior inching is considerably smaller when compared to anterior inching. As a result, since the

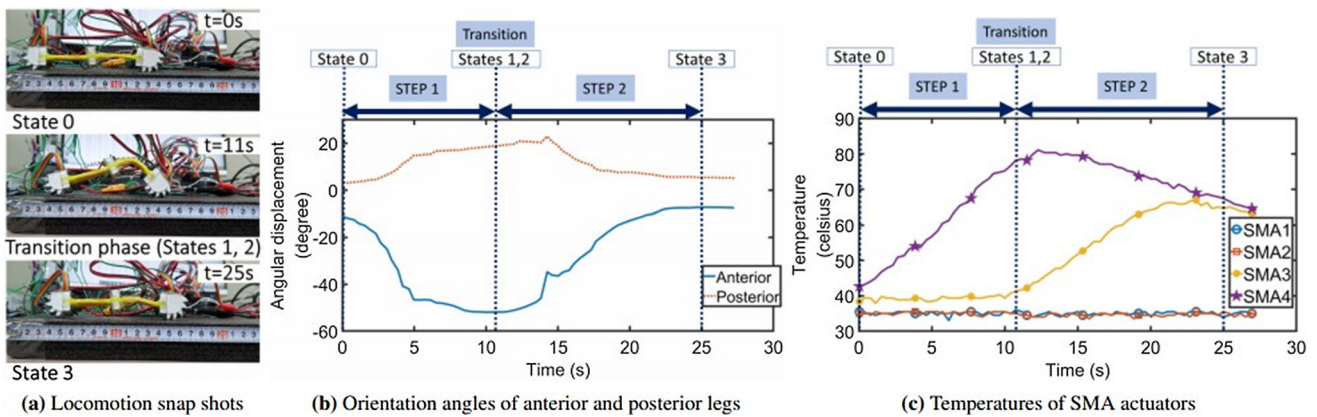


Fig. 13 Experimental results of anterior inching

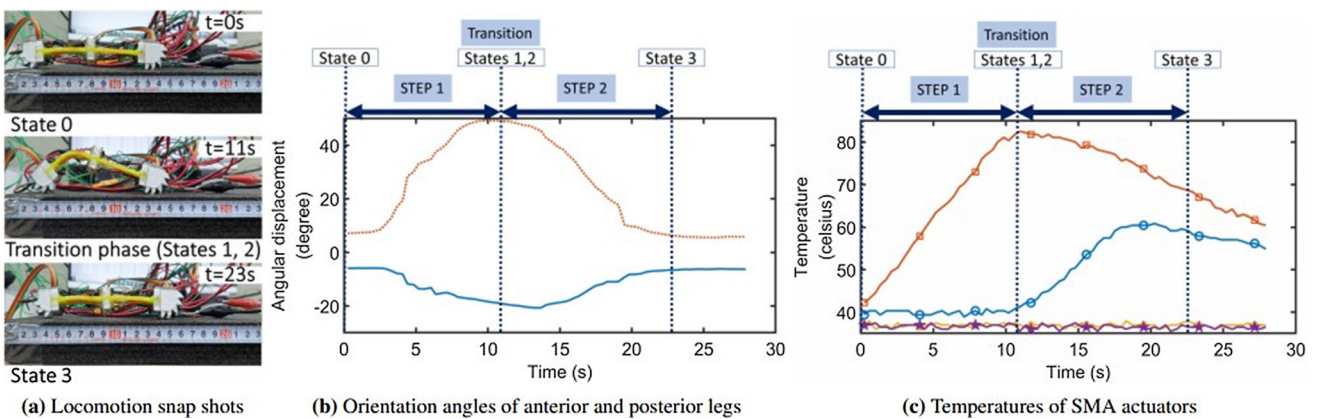


Fig. 14 Experimental results of posterior inching

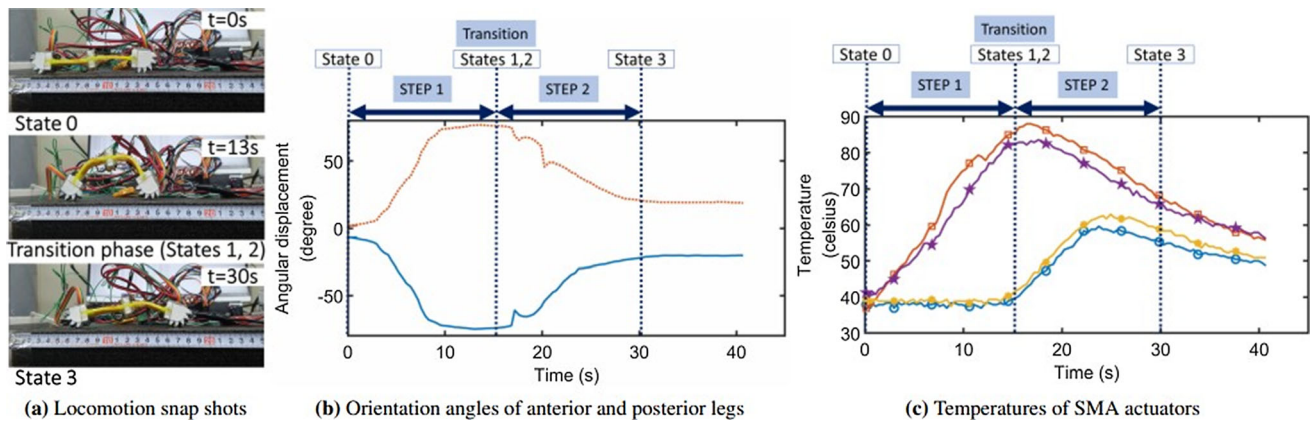


Fig. 15 Experimental results of fast inching

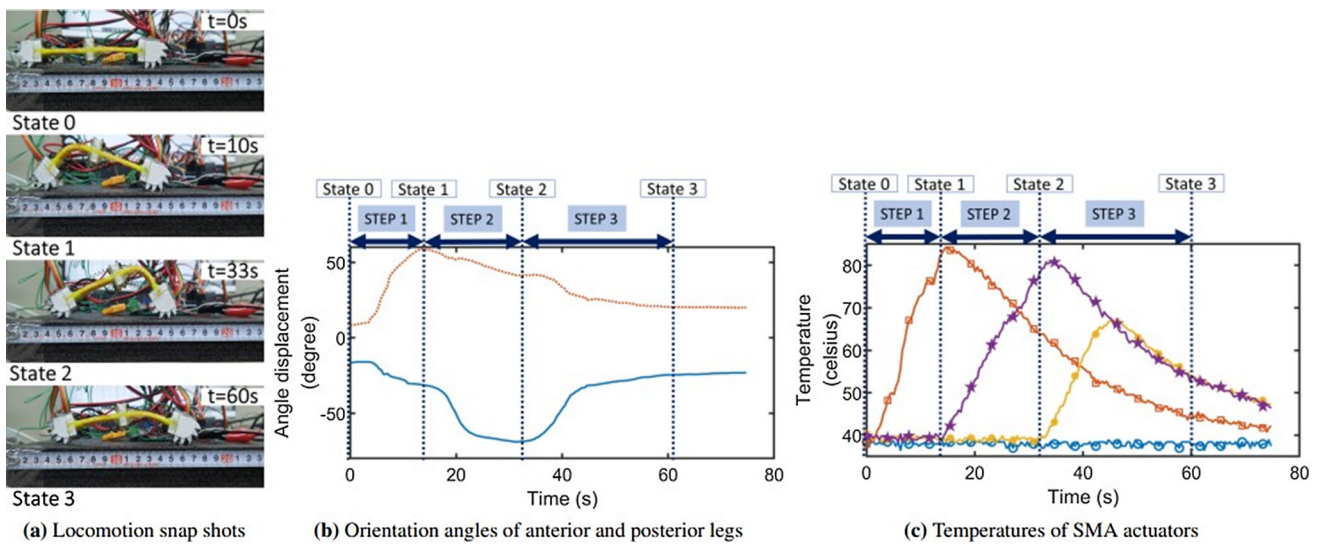


Fig. 16 Experimental results of basic crawling

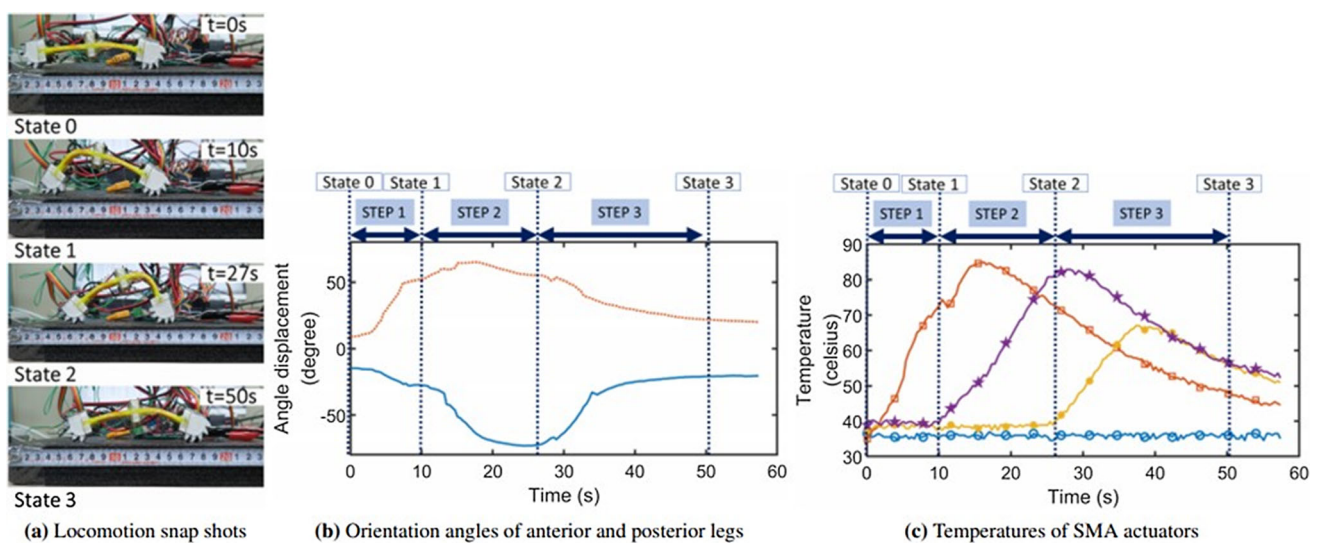


Fig. 17 Experimental results of faster crawling

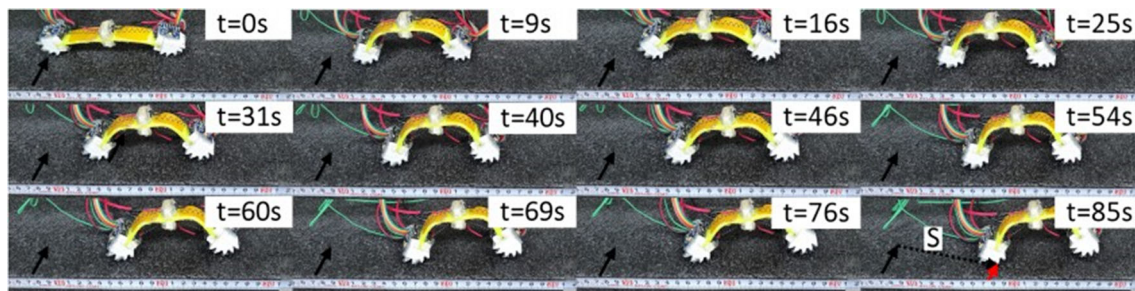


Fig. 18 Continuous fast inching locomotion

friction force is proportional to the normal force, the resulting friction force in posterior inching is significantly smaller than that in anterior inching. The orientation angles of the robot also indicate that the maximum bending occurs in the rear body segment. Furthermore, temperature changes in SMAs 1 and 2, shown in Fig. 14c, verify that the actuators are activated and deactivated as designed.

The travel velocity of the fast inching is fastest among the applied inching locomotion since the front and rear body segments are simultaneously contracted and then relaxed. Sequential snap shots obtained from the experiments of the fast inching are shown in Fig. 15a. SMAs 2 and 4 located at the bottom of the robot body are first activated simultaneously in Step 1 for contraction such that the robot is posed into an arch-like shape. Figure 15b shows the orientation angles of the front and rear ends of the robot body that change similar in magnitude but in opposite direction. This result also indicates a larger deflection is achieved in the robot as expected. The resulting travel distance of the rear leg increases significantly when compared to the other inching locomotion since the deflection of the whole body is larger. Through the state transition and in Step 2 for relaxation, SMAs 1 and 3 located above the body are activated simultaneously while SMAs 2 and 4 are turned off. Finally, all actuators are off in final State 3. Due to a larger deflection of the body, the contraction time and relaxation time for fast inching may increase slightly compared to the other locomotions. However, its travel speed increases considerably due to its larger travel distance per gait cycle. Additionally, the temperature measurements in Fig. 15c indicate that the SMA actuators are commanded as planned in each step. A similar magnitude of control inputs is applied to the front (SMAs 1 and 2) and rear (SMAs 3 and 4) actuator sets.

Crawling uses a symmetric gait pattern with a shorter wavelength compared to inching. Fig. 16a shows the basic crawling locomotion gaits sequentially obtained from the experiments. In Step 1, a half-sinusoidal gait pattern rises from the rear body while the front leg is locked, and the rear leg slips by using SMA 1. This gait pattern then propagates to the front body in Step 2 while the rear leg is

locked, and the front leg slips. Unlike the inching locomotion, SMA 1 is not used during the transition from Step 1 to Step 2 to avoid possible slipping of the rear leg in a backward direction. SMA 4 is then activated in Step 2 immediately after SMA 2 is off. Finally, the robot body is restored into its original pose in Step 3 while locking the rear leg. As a result, the travel distance of the robot is determined by the bending deflection of the robot body in Steps 1 and 2. Furthermore, this basic crawling is slightly modified to increase the locomotion speed by adjusting the actuation time in Step 2. To this end, we start to actuate

SMA 4 when the temperature of SMA 2 reaches around 70 °C below its transition temperature in Step 2. These faster crawling gaits are shown in Fig. 17. Note the rear leg in the faster crawling travels more distance than that in the basic crawling with a reduction in the run time by 3 seconds which can be observed in our results shown in Figs. 16 and 17. Our results confirm that the properly adjusted actuation time of the SMAs in locomotion can improve the travel velocity of the robot considerably. More importantly, our experimental results verify the gait patterns of the robot transit from the rear body to the front body in crawling as planned. The sequences of SMA actuation can be verified by referring to the temperature measurements in Figs. 16c and 17c. The orientation angles of the front and rear ends of the robot body are also shown in Figs. 16b and 17b. Note the orientations of the front end (or leg) are similar for both crawling locomotions whereas the orientations of the rear end (or leg) are slightly different due to the change in the actuation time of SMA 4.

Table 3 Actuator control plan for the undulating motion

STEP	SMA1	SMA2	SMA3	SMA4
0	OFF	OFF	OFF	OFF
1	OFF	OFF	OFF	ON
2	OFF	ON	OFF	OFF
3	OFF	OFF	ON	OFF
4	ON	OFF	OFF	OFF

Table 4 Locomotion characteristics (A.I: Anterior inching, P.I: Posterior inching, F.I: Fast inching, B.C: Basic crawling, F.C: Faster crawling)

Gait	Velocity, (cm/s)	Max. body height, (cm)	Distance, (cm)	Time, (s)
A.I	0.08	5	2	25
P.I	0.086	4.5	2	23
F.I	0.133	6.5	4.5	30
B.C	0.053	5.5	3.2	60
F.C	0.088	5	4.4	50

The locomotion characteristics are summarized in Table 3 by including the travel distance, elapsed time, linear velocity, and maximum achievable height of the robot per gait cycle. Fast inching provides the highest velocity of 0.16 cm/s as expected in our experiments while producing the highest height and longest travel distance. Anterior and posterior inching and faster crawling provide moderate velocities of 0.09 cm/s.

Basic crawling provides the lowest velocity of 0.053 cm/s. The velocity of the robot critically depends on the travel distance and the elapsed time per gait cycle. The travel distance of the robot is determined by the slip distance of the rear leg while the body of the robot is deflected, and the front leg is anchored. Crawling can provide a longer travel distance (4.1–4.5 cm) per cycle since it uses the propagation of an extended symmetric gait pattern. However, it also takes a much longer time (50–60 seconds) to complete this extended gait propagation. Furthermore, fast inching can provide a much longer travel distance (5.2 cm) per gait cycle since the body deflection of the robot can considerably be increased by bending the front and rear body segments simultaneously with a moderate cycle time (30 s). Our experimental results also suggest that the maximum body height should be considered for applications in a narrow space during locomotion such that the linear velocities should be lower by applying some locomotion with less deflection. The maximum height of the robot in fast inching is 5.2 cm which is the highest. However, anterior inching and faster crawling provide a lower maximum body height of 3.8 cm which may be the best for moving through narrow passages. Furthermore, our experimental results indicate the robot velocity depends on the friction force which is proportional to the normal force and friction coefficient. Our experiment results also verify that the ground friction force can be adjusted by rotating the legs with arch-shaped claws such that the legs can successfully be locked and unlocked as designed in our locomotion plan.

We verified the continuous inching locomotion by extending the cycle of inching gaits. Fig. 18 shows the experimental results of this continuous inching locomotion applying six gait cycles. This case demonstrates the continuous fast inching. The postures (i.e., orientation angles

of the front and rear legs) of the robot are slightly modified in each gait state to achieve a relatively faster motion. The posture during the transition between States 1 and 2 was determined to be 60° clockwise and counterclockwise for the front and rear legs, respectively. In State 3, the angles of the front and rear legs are increased from 0° to 45° clockwise and counterclockwise, respectively. According to this slight posture modification, a bang-bang controller is switched based on the orientation angles of the legs instead of the SMA temperatures. We also applied the same constant electrical power of 10 V and 2 A for this experiment, which was applied in the previous experiments. Note the travel distance of the robot is maximized when the robot starts to move from a straight posture. Since the robot posture of State 3 is not straight in this continuous locomotion, the travel distance per cycle becomes shorter compared to our previous results. The resulting average travel distance per cycle is about 1 cm.

5.4 Experimental results: undulatory locomotion

A full sinusoidal gait pattern is implemented to achieve a vertical undulatory locomotion shown in Fig. 4. In this locomotion, coordinated uses of locking and slipping of the front and rear legs are similar to those in the inching or crawling locomotion. However, robots can pose a full sinusoidal wave form in this undulatory locomotion. To achieve this undulatory motion, the desired orientation angles of the front and rear legs are predetermined. First, an angle feedback-based bang-bang controller is used in this case. Three gait cycles are used to demonstrate continuous locomotion.

Some animals such as snakes and eels are observed to use undulatory motion for their locomotion. Similarly, we applied the undulatory motion for locomotion of the robot in this study. A sinusoidal wave is used to generate this undulatory motion shown in Fig. 4. Table 4 shows the control plan for the SMA actuators to achieve this undulatory locomotion. In our case, a gait transition between sequential locomotion steps occurs when a corresponding leg rotates 30 degrees clockwise or counterclockwise according to our locomotion strategy.

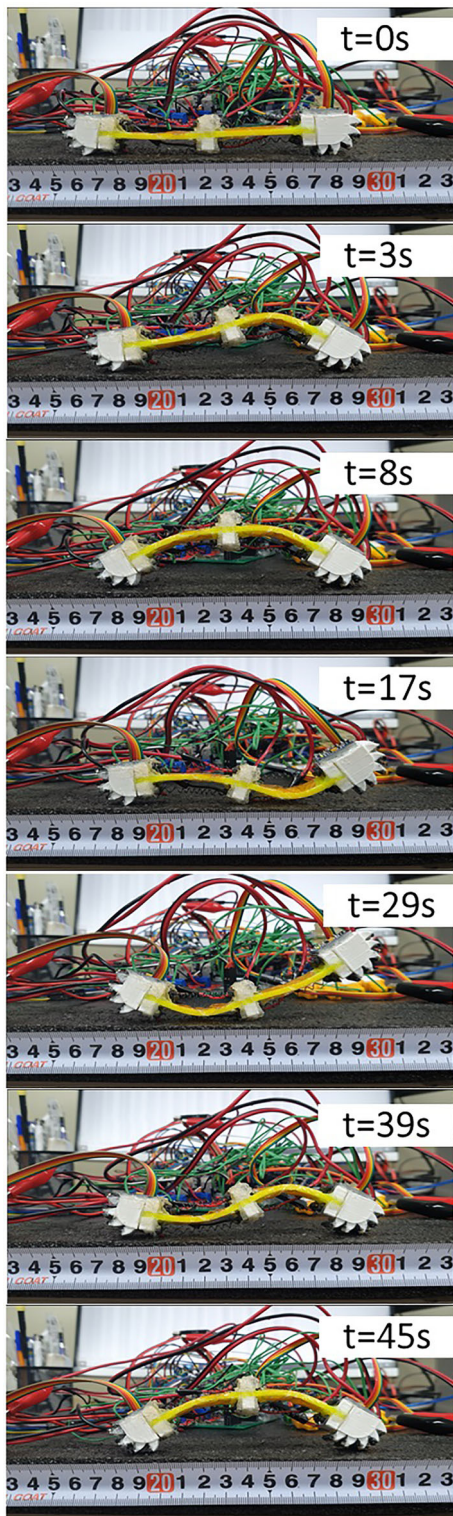


Fig. 19 Undulating motion of the Switch control system

Our experimental results, seen in Figs. 19, 20, 21, show that the vertical undulatory locomotion is achieved as designed. Sequential snap shots of the locomotion are shown in Fig. 19. Figure 20 shows the orientation angles of

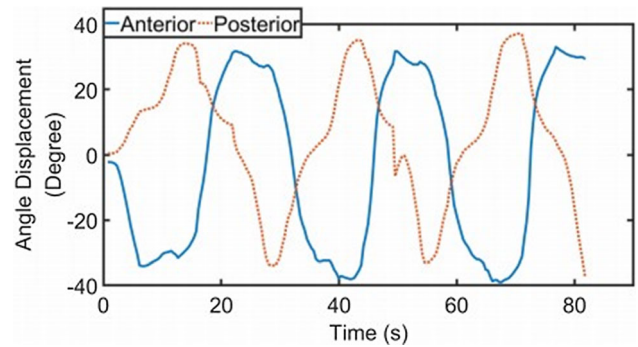


Fig. 20 Orientation angles of the legs in undulatory locomotion with the bang-bang control

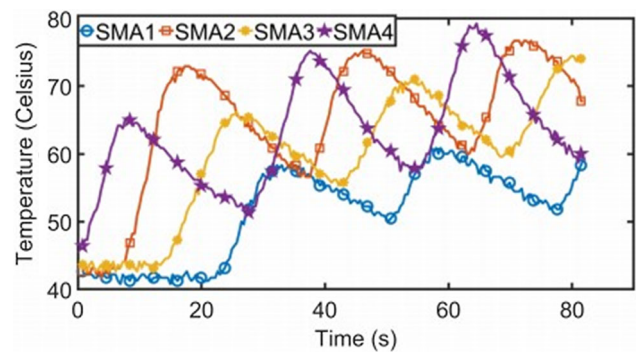


Fig. 21 SMA temperature in the undulatory locomotion with the bang-bang control

the front and rear legs (or body segments) in the undulatory locomotion applying the bang-bang control. These results verify that the sinusoidal gait patterns are executed as planned. Figure 21 then shows the measured temperatures of the SMA actuators in the undulatory locomotion. These temperature measurements confirm that control commands are provided to the SMA actuators sequentially as shown in Table 4. The temperature profiles of each cycle are similar. The SMA temperatures increase slightly after executing each gait cycle since natural convective cooling is slower. Travel speeds of the robot were experimentally obtained for a gait cycle of the undulatory locomotion. The resulting travel speeds are 0.034 cm/s for the first gait cycle, 0.038 cm/s for the second cycle, and 0.034 cm/s for the third cycle which are similar. Furthermore, we find States 0 and 2 are not necessarily required for locomotion even though these states are important in achieving a sinusoidal shape of the robot. As a result, the speed of this undulatory locomotion is relatively slower when compared to the other locomotions. Thus, only States 1 and 3 may be used to achieve a faster locomotion speed ignoring a full cycle of a sinusoidal shape.

6 Conclusions

This study presents a novel soft robot which can perform several different soft locomotions such as inching, crawling, and undulation. To achieve soft locomotion, the robot is designed to have a soft body and stick-slip mechanisms. As a result, the robot body is made of soft TPU material. Front and rear legs are then attached to the front and rear ends of the robot body similar to inchworms or caterpillars. Furthermore, arc-shaped claws are used to adjust the friction forces that are required for the stick-slip phenomenon in a locomotion strategy. Legs are designed to be locked and unlocked on the ground depending on the orientation of the legs. The inching, crawling, and undulation motions of the robot are achieved by applying sequentially coordinated control of four SMA springs. We verified our soft robot design, control algorithm, and locomotion strategies through various experiments. Our experimental results conform several different locomotions for the soft robot can be achieved with a simple bang–bang control. Fast inching can provide the highest speed of 0.133 cm/s. Inching and crawling can provide a speed of 0.08 cm/s. Vertical undulation may be used for locomotion even though it is relatively slower. Our results also verify that the locomotion performance of the robot can be adjusted easily by modifying gait cycle times or desired robot postures (position and orientation). Future work will study advanced control and locomotion algorithms to improve the locomotion performance for the soft robot.

Acknowledgements This research was mainly supported by the National Research Foundation of Korea (NRF) grant funded by the Korea government (MSIT) (No. 2021R1H1A2093798 and No. 2022R1A2C1011462). This research was also partially supported by “Regional Innovation Strategy (RIS)” through the National Research Foundation of Korea (NRF) funded by the Ministry of Education (MOE) (2021RIS-004). Further, the third and fifth authors are funded by the Brain Pool (BP) program by the National Research Foundation (NRF) with BP Grant (2019H1D3A1A01102998) and BP Grant (2019H1D3A1A01071124), respectively.

Data availability The authors declare that experimental and simulation data are available within the paper. Raw data will be available from the corresponding author upon reasonable request.

References

Brackenbury J (1999) Fast locomotion in caterpillars. *J Insect Physiol* 45:525–533

- Branyan C, Fleming C, Remaley J, Kothari A, Tumer K, Hatton R, Mengüç Y (2017) Soft snake robots: Mechanical design and geometric gait implementation. In: 2017 IEEE International Conference On Robotics And Biomimetics (ROBIO), pp. 282–289
- Coyle S, Majidi C, LeDuc P, Hsia K (2018) Bio-inspired soft robotics: material selection, actuation, and design. *Ext Mech Lett* 22:51–59
- Gillis G (1997) Anguilliform locomotion in an elongate salamander (Siren inter-media): effects of speed on axial undulatory movements. *J Exp Biol* 200:767–784
- Gordon M, Blickhan R, Dabiri J, Videler J (2017) Animal locomotion: physical principles and adaptations. CRC Press
- Hu W, Lum G, Mastrangeli M, Sitti M (2018) Small-scale soft-bodied robot with multimodal locomotion. *Nature* 554:81–85
- Joyce E, Pan Y (2019) A fully three-dimensional printed inchworm-inspired soft robot with magnetic actuation. *Soft Rob* 6:333–345
- Ju Y, Hu R, Xie Y, Yao J, Li X, Lv Y, Han X, Cao Q, Li L (2021) Reconfigurable magnetic soft robots with multimodal locomotion. *Nano Energy* 87:106169
- Koh J, Cho K (2009) Omegabot: Biomimetic inchworm robot using SMA coil actuator and smart composite microstructures (SCM). In: 2009 IEEE International Conference On Robotics And Biomimetics (ROBIO), pp. 1154–1159
- Lin H, Leisk G, Trimmer B (2011) GoQBot: a caterpillar-inspired soft-bodied rolling robot. *Bioinspir Biomim* 6:026007
- Rus D, Tolley M (2015) Design, fabrication and control of soft robots. *Nature*: 467–475
- Tang X, Li K, Liu Y, Zhou D, Zhao J (2019) A soft crawling robot driven by single twisted and coiled actuator. *Sens Actu Phys* 291:80–86
- Trimmer B, Lin H, Baryshyan A, Leisk G, Kaplan D (2012) Towards a biomorphic soft robot: design constraints and solutions. In: 2012 4th IEEE RAS & EMBS International Conference On Biomedical Robotics And Biomechanics (BioRob), pp. 599–605
- Ueno S, Takemura K, Yokota S, Edamura K (2014) Micro inchworm robot using electro-conjugate fluid. *Sens Actu Phys*: 36–42
- Umedachi T, Kano T, Ishiguro A, Trimmer B (2016) Gait control in a soft robot by sensing interactions with the environment using self-deformation. *R Soc Open Sci* 3:160766
- Wu S, Ze Q, Dai J, Udipi N, Paulino G, Zhao R (2021) Stretchable origami robotic arm with omnidirectional bending and twisting. *Proc Natl Acad Sci* 118:e2110023118
- Yamakita M, Kamamichi N, Kozuki T, Asaka K, Luo Z (2005) A snake-like swimming robot using IPMC actuator and verification of doping effect. In: 2005 IEEE/RSJ International Conference on Intelligent Robots And Systems, pp. 2035–2040

Publisher's Note Springer Nature remains neutral with regard to jurisdictional claims in published maps and institutional affiliations.

Springer Nature or its licensor (e.g. a society or other partner) holds exclusive rights to this article under a publishing agreement with the author(s) or other rightsholder(s); author self-archiving of the accepted manuscript version of this article is solely governed by the terms of such publishing agreement and applicable law.